ChemComm

Cite this: *Chem. Commun.*, 2012, **48**, 4695–4697

www.rsc.org/chemcomm

COMMUNICATION

Micelles based on gold-glycopolymer complexes as new chemotherapy drug delivery agents†

Samuel Pearson, Wei Scarano and Martina H. Stenzel*

Received 22nd January 2012, Accepted 9th March 2012
DOI: 10.1039/c2cc30510k

Polymeric versions of deacetylated auranofin, a gold complex with a sugar ligand, were prepared by post-modifying RAFT glycopolymers. Micellisation of a block copolymer containing pendant Au(I) units produced nanoparticles with an increased anti-proliferative effect against OVCAR-3 human ovarian carcinoma cells.

Auranofin (**1**, Scheme 1) is a gold(I) complex which has been used extensively to treat rheumatoid arthritis for the past four decades,[1] but more recently its activity against several tumour cell lines has generated great interest for its potential use as a chemotherapy agent.[2]

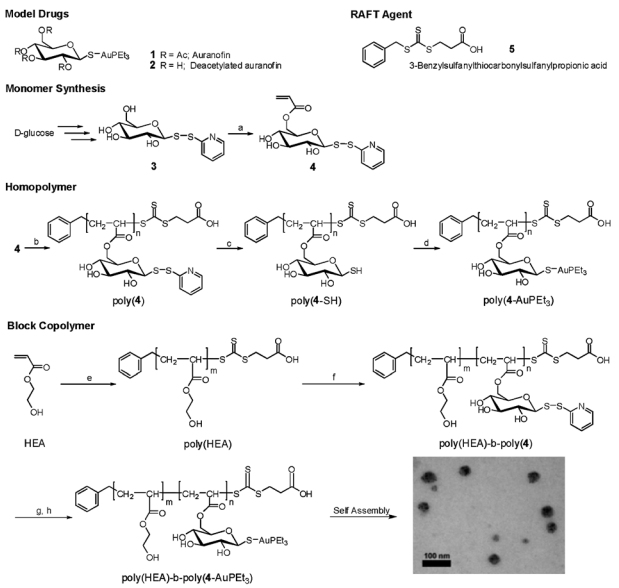

Scheme 1 (a) Vinyl acrylate, Novozym 435, acetone, 5 Å molecular sieves, 50 °C, 5 days; (b) Chlorobenzene, AIBN, RAFT agent **5**, 60 °C, 7 h; (c) DMSO, DTT, 0 °C, 24 h; (d) DMAc, NEt_3, $AuPEt_3$, 0 °C, 24 h; (e) RAFT agent **5**, DMF, AIBN, 60 °C, 70 min; (f) DMF, AIBN, **4**, 60 °C, 9 h; (g) DMAc, DTT, 0 °C, 24 h; (h) DMAc, TEA, $AuPEt_3Cl$, 0 °C, 24 h. Inset; TEM image of the self-assembled poly(HEA)-*b*-poly(**4**-$AuPEt_3$).

Centre for Advanced Macromolecular Design, University of New South Wales, Sydney, Australia. E-mail: M.Stenzel@unsw.edu.au; Fax: + 61-2-93856250; Tel: + 61-2-93854344

† Electronic supplementary information (ESI) available: Syntheses, NMR and TGA characterisations, details on chain transfer experiment, complexation efficiency calculations. See DOI: 10.1039/c2cc30510k

Auranofin has been identified as one of the most potent and selective inhibitors of the mitochondrial protein thioredoxin reductase,[3] an important new drug target central to the progression of several chronic diseases including rheumatoid arthritis and some cancers.[4] Increased expression of thioredoxin reductase is linked to proliferant tumour cell growth, suppressed apoptosis, and resistance to conventional chemotherapy.[5] Conversely, inhibition of thioredoxin reductase causes a build-up of hydrogen peroxide and oxidized thioredoxins which act on a variety of targets within the mitochondria to induce cell death.[6] Direct stimulation of this mitochondrial cell death pathway reduces the cells' ability to establish resistance, potentially overcoming a key challenge presented by conventional chemotherapy.[7] For example, both normal and cisplatin-resistant human ovarian cancer cells have been shown to be highly susceptible to auranofin, whereas cisplatin was ineffective against the resistant cell line.[8] Auranofin therefore displays promising attributes as a potential chemotherapy drug able to overcome the resistance and selectivity problems which plague conventional chemotherapy agents.

Despite its pronounced antitumour activity *in vitro*,[9] however, auranofin is highly reactive towards protein thiols and undergoes rapid ligand displacement reactions *in vivo*,[10] primarily with serum albumin.[11] This rapid ligand displacement severely limits the applicability of auranofin as an antitumour agent *in vivo*. A range of alternative Au(I) complexes with thiol-free ligands such as chelating diphosphines have demonstrated stability in the presence of thiols[12] and high activity against several human cisplatin-resistant ovarian cancer cell lines, but activity closely correlated with *in vivo* hepatotoxicity[13] and reduced solubility.[14]

Rather than seeking alternative complexes, we propose that a micellar system containing pendant auranofin-like groups in the core and a hydrophilic shell will offer the dual advantages of protecting the auranofin from interacting with serum proteins, and accumulating preferentially in tumour tissue *via* the enhanced permeability and retention effect[15] which will aid selective uptake by tumour cells.

We have designed a glycomonomer which mimics the structure of deacetylated auranofin (**2**, Scheme 1) whose antitumour potency is comparable to that of auranofin.[16] The monomer (**4**, Scheme 1) was synthesized in 6 steps from D-glucose with the anomeric thiol protected with a pyridyl disulfide group, and an enzymatic approach chosen to regioselectively

functionalise the 6-position of the sugar with an acrylate group.[17] This reaction using vinyl acrylate was catalysed by Novozym 435, a lipase derived from *Candida antarctica*, and 5 Å molecular sieves were used to absorb the acetaldehyde byproduct and thereby remove it from the equilibrium to maximise the yield (see ESI†).[18] RAFT polymerization was identified as a suitable technique to polymerize monomer **4** due to its robustness in the presence of many functional groups and the non-toxicity of most RAFT agents.[19] Polymerization of **4** was performed using the trithiocarbonate RAFT agent 3-benzylsulfanylthiocarbonylsulfanylpropionic acid (**5**, Scheme 1) to generate a homopolymer (poly(**4**), Scheme 1) capable of forming a polymeric analogue of deacetylated auranofin. DMF and DMAc were effective solvents for **4**, but some yellowing of the polymerization solution at longer reaction times encouraged a switch to chlorobenzene given that the solubility of **4** was limited in other more commonly used polymerization solvents such as methanol, ethanol, isopropanol, acetone, and DMSO. After a polymerization time of 7 h ($[M]_0$ = 0.8 M) a conversion of around 40% was reached (Fig. S1, ESI†).

The resulting homopolymer of **4** was reasonably well defined ($M_{n,theor}$ = 14.1 kDa, PDI 1.49) with slight broadening attributed to side reactions involving the pyridyl disulfide protecting group. A chain transfer experiment using its disulfide precursor (**3**, Scheme 1) gave a chain transfer constant of 2.8×10^{-3} for the disulfide group (Fig. S2–S4, ESI†), which is significant enough to influence the breadth of the molecular weight distributions. However, a marked narrowing of the molecular weight distribution to a PDI of 1.23 and a corresponding shift to higher molecular weight (Fig. 1) was achieved when the pyridyl disulfide groups were cleaved using D,L-dithiothreitol (DTT) to generate free thiols on the sugar units, indicating that some broadening of poly(**4**) might also have been the result of disulfide bridge formation during the polymerization. The shift to higher molecular weight suggests that the thiol-containing polymer possesses a higher hydrodynamic radius than its precursor.

The thiol-containing polymer poly(**4**-SH) was purified by two precipitations into cold EtOAc before the isolated powder was immediately dissolved in DMAc and purged with nitrogen to prevent disulfide formation before the subsequent complexation. It was also important to ensure no DTT was present prior to the addition of $AuPEt_3Cl$ to avoid side reactions in the following step. Triethylamine (TEA) was added to deprotonate the anomeric thiols, and a degassed solution containing 1.2 equivalents of $AuPEt_3Cl$ in DMAc was added slowly under a nitrogen atmosphere. The complexed polymer poly(**4**-$AuPEt_3$) was purified by three precipitations into cold EtOAc (in which $AuPEt_3Cl$ is soluble). The complexation was accompanied by a shift towards higher molecular weight as determined by SEC (Fig. 1).

^{1}H NMR spectroscopy (Fig. 2) showed the disappearance of pyridyl proton peaks in the final complex, demonstrating that the cleavage of the pyridyl disulfide protecting groups occurred almost quantitatively, and the emergence of multiplets at 1.87 ppm and 1.11 ppm confirmed the presence of the ethyl groups of the triethylphospine-containing Au(I) units. Proton peaks were assigned with the aid of {^{1}H–^{13}C}HSQC correlation measurements (Fig. S5–S6, ESI†). In addition, the ^{31}P NMR spectrum shows a single broad peak at 38.92 ppm characteristic of the triethyl phosphine ligands distributed along the polymer (Inset of Fig. 2b), with the breadth arising due to the slightly different electronic environments experienced by each pendant group. With a phosphorous chemical shift very close to that of **2** (Inset of Fig. 2c; the slight difference in chemical shift attributable to the differing NMR solvents) and an absence of impurity peaks, it is confirmed that the complexation affords the desired product efficiently with no side reactions.

Thermogravimetric analysis (TGA) of poly(**4**-$AuPEt_3$) using air as the furnace gas (Fig. S7, ESI†) generated a residual mass of 29% at 800 °C corresponding to elemental gold derived from the polymeric complex. An identical analysis of the poly(**4**-SH) precursor confirmed that all mass contributed by the polymer was oxidized to leave zero residual mass. Assuming that every pendant group in poly(**4**-SH) contained a free thiol to which Au(I) could complex, the efficiency of the complexation step was 72% (see ESI† for calculations).

After a successful proof of concept in complexing $AuPEt_3Cl$ to the thiol-bearing poly(**4**-SH) to generate a polymeric form of **2**, the strategy was extended to a block copolymer system in which a trithiocarbonate macroRAFT agent of 2-hydroxyethyl acrylate (HEA) was chain extended with **4** to produce a poly(HEA)-*b*-poly(**4**) block copolymer (Scheme 1).

The block copolymer displayed a slight broadening of the molecular weight distribution compared to the poly(HEA)

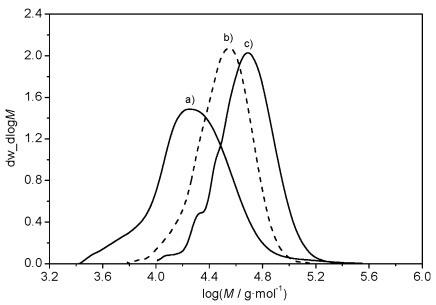

Fig. 1 SEC traces of (a) Poly(**4**), $M_{n,SEC}$ = 15.0 kDa, PDI = 1.49; (b) Poly(**4**-SH), $M_{n,SEC}$ = 28.2 kDa, PDI = 1.23; and (c) Poly(**4**-$AuPEt_3$), $M_{n,SEC}$ = 40.2 kDa, PDI = 1.24.

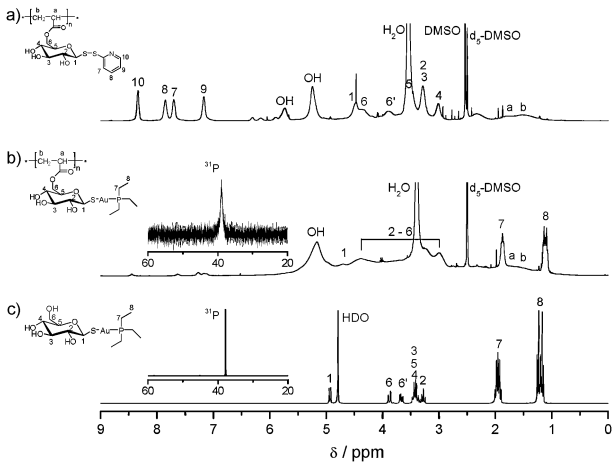

Fig. 2 ^{1}H NMR spectra of (a) Poly(**4**) in d_6-DMSO; (b) Poly(**4**-$AuPEt_3$) in d_6-DMSO; and (c) Deacetylated auranofin **2** in D_2O; ^{31}P NMR spectra of (b) and (c) are inset.

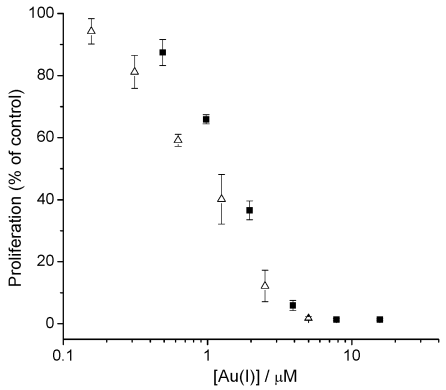

Fig. 3 Proliferation of OVCAR-3 human ovarian carcinoma cells in the presence of **2** (closed squares) and poly(HEA)-*b*-poly(**4**-AuPEt$_3$) (open triangles) as a function of Au(I) content.

macroRAFT agent, but after purification by dialysis and cleavage of the pyridyl disulfide groups using DTT, the molecular weight distribution narrowed and shifted to higher molecular weight in a similar fashion to the homopolymer system (Fig. S8, ESI†). Complexation of AuPEt$_3$Cl to the purified block copolymer using the same approach generated an amphiphilic block copolymer with the AuPEt$_3$ complexed to the thiol units of the pendant sugars. Based on TGA analysis (Fig. S9, ESI†), the block copolymer contained 20% gold by mass which corresponds to a loading efficiency of approximately 74%. It was hoped that the introduction of the AuPEt$_3$ group would render the Au(I)-containing block hydrophobic relative to the readily water soluble poly(HEA) block and thereby encourage self-assembly into a core-shell structure in an aqueous environment. Indeed, controlled addition of water to a DMSO solution of the pure block copolymer followed by dialysis against water produced micelles with a mean diameter of approximately 75 nm by dynamic light scattering (DLS, Fig. S10, ESI†). Transmission electron microscopy (TEM) confirmed the presence of spherical structures containing distinct gold-rich domains which strongly scattered the electron beam and generated excellent contrast in the images (Inset, Scheme 1).

The activity of the micellar poly(HEA)-*b*-poly(**4**-AuPEt$_3$) system against tumour cells was evaluated by measuring the proliferation OVCAR-3 human ovarian carcinoma cells in the presence of either the discrete drug **2** or its micellar analogue at increasing concentrations (Fig. 3). It was not deemed appropriate to use either poly(HEA)-*b*-poly(**4**) or poly(HEA)-*b*-poly(**4**-SH) precursors as negative controls, because neither the pyridyl disulfide groups nor the free thiols in each would constitute a valid reference in the same way that an unloaded micelle serves as the negative control for a micelle system physically loaded with a drug. The dose-response curves of cell proliferation as a percentage of the control (cells incubated with medium only) demonstrate similar profiles for **2** and poly(HEA)-*b*-poly(**4**-AuPEt$_3$), with poly(HEA)-*b*-poly(**4**-AuPEt$_3$) actually exhibiting slightly higher activity compared to **2**. Indeed, regression analysis of the two curves indicates that the IC_{50} inhibitory concentration for poly(HEA)-*b*-poly(**4**-AuPEt$_3$) is 0.94 μM (based on the concentration of Au(I) in the system) and the value for **2** is 1.51 μM. Considering that **2** is one of the most potent known compounds for inducing cell death *via* direct interaction with the mitochondria, higher activity in our micellar system is very promising for the potential development of this polymer-gold system into a chemotherapy treatment.

The increased activity can be explained *via* the different route of cell entry. Whilst low molecular weight drugs such as **2** diffuse through the cell membrane, nanoparticles are taken up by endocytosis. This route not only provides a more efficient entry pathway, but also offers the possibility of by-passing the drug resistance mechanism induced by small molecules.[20]

It has been demonstrated that glycopolymers bearing protected thiosugar units can be efficiently converted to polymeric Au(I) complexes. In micellar form, the block copolymer system displayed higher activity against OVCAR-3 cells than its small molecule analogue, offering a promising alternative delivery mechanism which may overcome the stability and toxicity issues faced by discrete Au(I) based chemotherapeutics. We are currently investigating the protection offered by the micellar system in preventing ligand displacement with serum proteins, and the controlled synthesis of related polymer-gold systems.

MS thanks the Australian Research Council for financial support.

Notes and references

1 C. Gaujoux-Viala, J. S. Smolen, R. Landewé, M. Dougados, T. K. Kvien, E. M. Mola, M. Scholte-Voshaar, P. van Riel and L. Gossec, *Ann. Rheum. Dis.*, 2010, **69**, 1004.
2 C. F. Shaw, *Chem. Rev.*, 1999, **99**, 2589.
3 (*a*) S. Gromer, L. D. Arscott, C. H. Williams, R. H. Schirmer and K. Becker, *J. Biol. Chem.*, 1998, **273**, 20096; (*b*) S. Urig, K. Fritz-Wolf, R. Réau, C. Herold-Mende, K. Tóth, E. Davioud-Charvet and K. Becker, *Angew. Chem., Int. Ed.*, 2006, **45**, 1881.
4 K. Becker, S. Gromer, R. H. Schirmer and S. Müller, *Eur. J. Biochem.*, 2000, **267**, 6118.
5 A. Burke-Gaffney, M. E. J. Callister and H. Nakamura, *Trends Pharmacol. Sci.*, 2005, **26**, 398.
6 M. P. Rigobello, A. Folda, M. C. Baldoin, G. Scutari and A. Bindoli, *Free Radical Res.*, 2005, **39**, 687.
7 V. R. Fantin and P. Leder, *Oncogene*, 2006, **25**, 4787.
8 C. Marzano, V. Gandin, A. Folda, G. Scutari, A. Bindoli and M. P. Rigobello, *Free Radical Biol. Med.*, 2007, **42**, 872.
9 C. K. Mirabelli, R. K. Johnson, D. T. Hill, L. F. Faucette, G. R. Girard, G. Y. Kuo, C. M. Sung and S. T. Crooke, *J. Med. Chem.*, 1986, **29**, 218.
10 S. Ahmad, A. A. Isab, S. Ali and A. R. Al-Arfaj, *Polyhedron*, 2006, **25**, 1633.
11 J. R. Roberts, J. Xiao, B. Schliesman, D. J. Parsons and C. F. Shaw, *Inorg. Chem.*, 1996, **35**, 424.
12 S. J. Berners-Price and A. Filipovska, *Aust. J. Chem.*, 2008, **61**, 661.
13 J. J. Liu, P. Galettis, A. Farr, L. Maharaj, H. Samarasinha, A. C. McGechan, B. C. Baguley, R. J. Bowen, S. J. Berners-Price and M. J. McKeage, *J. Inorg. Biochem.*, 2008, **102**, 303.
14 M. J. McKeage, S. J. Berners-Price, P. Galettis, R. J. Bowen, W. Brouwer, L. Ding, L. Zhuang and B. C. Baguley, *Cancer Chemother. Pharmacol.*, 2000, **46**, 343.
15 A. K. Iyer, G. Khaled, J. Fang and H. Maeda, *Drug Discovery Today*, 2006, **11**, 812.
16 E. R. T. Tiekink, *Crit. Rev. Oncol. Hematol.*, 2002, **42**, 225.
17 O.-J. Park, D.-Y. Kim and J. S. Dordick, *Biotechnol. Bioeng.*, 2000, **70**, 208.
18 Y. Li and D. G. Rethwisch, *Biotechnol. Bioeng.*, 2002, **79**, 15.
19 A. Gregory and M. H. Stenzel, *Expert Opin. Drug Delivery*, 2011, **8**, 237.
20 J. Zastre, J. Jackson, M. Bajwa, R. Liggins, F. Iqbal and H. Burt, *Eur. J. Pharm. Biopharm.*, 2002, **54**, 299.